A Pulsed Plasma Thruster Using Mercury Propellant: A Late-1960s Project at the Royal Aerospace Establishment, Farnborough

IEPC-2007-290
Presented at the 30th International Electric Propulsion Conference, Florence, Italy
September 17-20, 2007

David G Fearn*
EP Solutions, 23 Bowenhurst Road, Church Crookham, Fleet, Hants, GU62 6HS, UK

Abstract: During the late 1960s and early 1970s a pulsed plasma thruster (PPT) was developed by the Space Department of the Royal Aerospace Establishment (RAE) at Farnborough. A conventional rail gun concept was adopted, although it was considered that there would be advantages in using the same propellant as an ion thruster being developed simultaneously; this was mercury. Several diagnostic instruments were utilised in characterising the thruster, including a thrust balance, high speed photography and a variety of plasma probes. Considerable success was achieved in operating the device over a wide range of conditions. As well as presenting these performance data, the paper illustrates the plasma structures observed photographically, and also examines in more detail the Langmuir probe results. The plasma velocities, when combined with momentum transfer data, suggested that the overall efficiency was between 3% and 25%. However, the total amount of mercury used was far greater than these data suggested, indicating that a great deal of evaporation took place after the acceleration process was complete. Thus the actual propellant utilisation efficiency was very low, as was the fully corrected total efficiency.

I. Introduction

During the mid-1960s serious consideration was given by the Space Department of the Royal Aerospace Establishment (RAE) at Farnborough to the development of a gridded ion thruster using mercury propellant. Experimental work commenced in 1967[1] and this eventually led to the T5 and T6 thrusters[2,3] now available from QinetiQ, and which use xenon propellant. Incidentally, QinetiQ evolved from RAE and other UK research establishments via a long and complicated process. In parallel with the initial development of the ion thruster, the other propulsion requirements of a typical spacecraft were investigated, with the result that a separate low-thrust device was deemed to be required for attitude control. It was therefore decided to develop a pulsed plasma thruster (PPT) for this application, and that the rail gun concept extensively studied elsewhere with considerable success should be adopted. However, it was considered that there would be significant advantages in using the same propellant as the ion thruster. Thus this device became unique in employing mercury for this purpose.

In justifying this programme, it can be stated that it was well known in the mid-1960s that electric propulsion systems become more competitive for attitude control and station-keeping tasks as satellite lifetimes increase, owing to the high exhaust velocities attainable with electromagnetic or electrostatic acceleration processes. These high velocities allow a given total impulse to be provided with a considerable saving of propellant mass when compared with conventional gas-jet systems. The high initial mass of the thruster and its power supply becomes relatively unimportant as mission time is extended to several years.

At that time, it was thought that many different types of thruster were suitable for these tasks, including ion thrusters using both mercury[4] and cesium[5] propellant, and a variety of pulsed plasma devices[6-8]. The latter were

* Sole Proprietor; dg.fearn@virgin.net

considered to have the significant advantage of requiring zero stand-by power, whilst being able to respond almost instantaneously to a demand for thrust. This rapid response was deemed to be of great importance in certain special applications, such as precise drag compensation[9]. Pulsed plasma devices were presumed to be simpler to construct and to operate than ion thrusters, requiring less complex power supplies and control circuitry, and were able to produce minute impulse bits with durations as short as 1 μs. Limitations were thought to include poor electrical and mass utilisation efficiencies, but the former was not considered to be serious in applications where large amounts of power were available, and the latter did not appear to cause an unacceptable mass increase for most missions of interest.

This paper concerns the development of this PPT, which had the initial aim of achieving, with repetitive firing, a thrust of about 0.5 mN (50 dynes in 1968 currency) and an electrical efficiency exceeding 10%. It was also intended to examine the feasibi!ity of producing a device suitable for practical attitude control in space. Development of the PPT commenced in parallel with the initial ion thruster laboratory programme[1] and continued for about 4 years, utilising a 1 m diameter vacuum chamber evacuated by a 36 inch diameter oil diffusion pump. The ultimate vacuum was in the 10^{-7} Torr range.

A double rail accelerator concept was chosen for simplicity and to avoid the current sheet instabilities often found in coaxial devices. Mercury propellant was used to achieve commonality with the ion thruster programme; other benefits included its ease of storage and high atomic weight. Gaseous propellants, although capable of being more accurately injected into a thruster, were not thought suitable due to storage difficulties and the potential unreliability of fast gas valves.

As described below, initially the programme placed most emphasis on observations of the acceleration of the plasma between the rail electrodes and on obtaining an understanding of the processes responsible[10]. In addition, the mechanism of the trigger discharge was also investigated[11]. This work was followed by a study of the exhaust plasma using a calorimeter, Langmuir probes and image converter high-speed photography. A sensitive thrust balance was also designed and constructed, and data obtained from this and the other techniques allowed the electrical and mass utilisation efficiencies to be evaluated.

II. The Thruster

The thruster is shown diagrammatically in Fig l. The 0.5 cm dia 10 cm long stainless steel electrodes were mounted on a boron nitride breech and diverged by 15° to maximise their total inductance while keeping their separation small at the breech to assist the triggering process. They were sandwiched between a pair of flat insulating plates, boron nitride being used on one side and, to allow photography of the plasma, glass on the other.

The mercury propel1ant was fed to a 1 mm dia hole in the breech by an MHD pump. The meniscus achieved a stable position in this hole, the surface tension force being balanced by the pump. A pointed trigger pin was placed about 1 mm above the meniscus and was connected to a 0.01 μF capacitor, C_T, charged through resistor R_T. The triggering system was isolated from earth by resistor R_E.

A low inductance capacitor of 1.0 or 1.3 μF was connected to the rails by a strip transmission line. Calibrated Rogowski coils were employed to measure the current in this transmission line and in the trigger circuit.

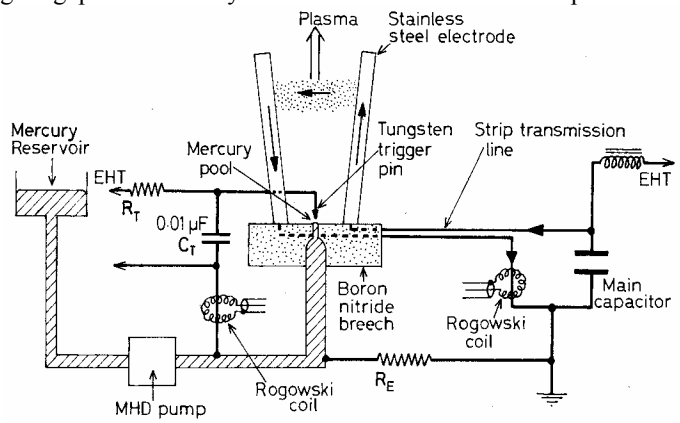

Figure 1. Schematic diagram of the rail thruster.

III. The Plasma Production and Acceleration Process

A. Propellant Injection and Triggering System

An auxiliary discharge between the trigger pin and mercury meniscus was used to both inject prope1lant into the space above the breech and to produce sufficient ionisation to trigger the main discharge[11]. For a given pin-meniscus separation, there existed a definite breakdown potential, V_T, and when this was reached as C_T was charged

the trigger discharge occurred. The Rogowski coil showed that the 2.5 MHz vacuum arc discharge had a peak current of 560 A when V_T = 4 kV. It was possible to vary V_T by changing the pin-meniscus separation, and continuous application of the charging voltage to R_T allowed repetitive triggering at a frequency determined by V_T and the time constant $R_T C_T$.

The arc vaporised a small quantity of mercury from the meniscus, about 0.3 µg/discharge at 2 kV. This was ionised by the oscillatory current, expanded to fill the space between the electrodes and, after about 1 µs, allowed the main discharge to be initiated.

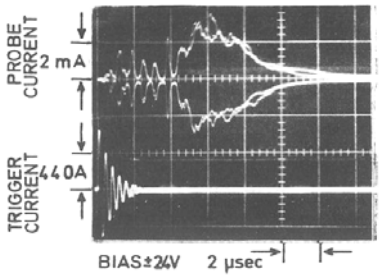

Figure 2a. Overlaid Langmuir probe traces 4 cm from the breech, with V_T = 5 kV.

Measurements were made of the electron number density, n_e, and temperature, T_e, of this p1asma, using a double Langmuir probe[12] cleaned by ion bombardment at frequent intervals. A typical oscillogram of the probe current is shown in Fig.2a, and a voltage-current characteristic in Fig.2b. This and similar characteristics taken at different positions and times indicated that T_e fell from about 2×10^4 K close to the breech to 1.3×10^4 K at 4 cm, whilst n_e was 3×10^{13} cm^{-3} at 2 cm and 4 µs after discharge initiation, and 7×10^{12} cm^{-3} at 4 cm and 8 µs.

The oscillograms of probe current contained smooth regular peaks before the arrival of the main trigger plasma at the probe position (Fig 2a). These were shown to be genuine conduction currents and it is proposed that they were due to the acceleration of electrons away from the discharge region at a velocity of about 6 cm/µs. This occurred only on those half-cycles of the discharge when the trigger pin was positive, as only on those occasions was the electric field in the correct direction.

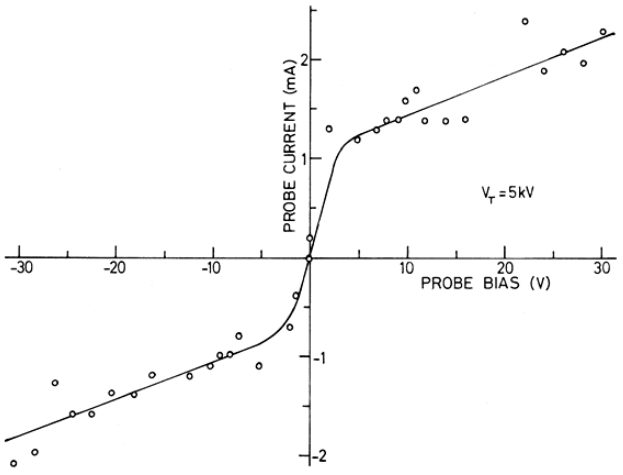

Figure 2b. Langmuir probe characteristic 4 cm from the mercury pool and 8 µs after discharge initiation.

The above values of n_e and T_e were consistent with a main discharge initiation mechanism proposed earlier for electrodes immersed in shock tube plasmas[13]. It is suggested that, in the absence of cathode emission, the currents to the electrodes from the injected plasma were small, being controlled by ion mobility. The potential drop across the plasma was therefore also small and most of the applied voltage appeared across the cathode sheath, that across the anode sheath being only sufficient to reduce the net electron current to the anode to balance the cathode ion current[11]. Assuming the sheath to be of the order of a Debye length thick[14], typically 2×10^{-4} cm, the electric field in the sheath was about 5×10^6 to 10^7 V/cm. This was adequate to cause field emission from isolated irregularities or impurity centres. After its initiation, this electron emission was maintained by a non-thermionic cathode spot process in which the required electric field resulted from the space charge of the cathode ion current[13]. Experiments in which changes of cathode material and configuration and of trigger discharge energy were made and were consistent with this mechanism.

It should be pointed out that estimates of plasma mean free paths revealed that the probe seriously perturbed the plasma[15], because it was much larger than assumed in the theory used in the analysis of the voltage-current characteristics. Although the magnitude of the perturbation was probably reduced by the plasma flow[12], the values of n_e given above were too small. Consequently the Debye length was shorter than previously estimated and the electric field in the sheath was greater.

Although this triggering system functioned satisfactorily, after long periods of operation reproducibility deteriorated. This problem was solved by the use of a two-stage process. In this the pin-meniscus discharge was initiated by a small amount of plasma ejected from the interface between the mercury pool and a refractory semiconductor (Fig 3) on applying a 400 V pulse to the latter. It was shown that the mechanism by which this initial

burst of plasma was produced was similar to that ascribed to certain ignitron discharges[16]. This process, using silicon carbide rather than boron carbide, allowed 20 discharges/s to be maintained indefinitely.

B. Plasma Acceleration

The plasma acceleration resulting from the interaction of the discharge current through the plasma with the magnetic field between the electrodes was studied by image converter photography and magnetic probes, while the current was monitored using Rogowski coils.

A series of 100 ns exposure photographs of the plasma produced by a 2 kV discharge was taken, using an image converter camera, at the times related to the current waveform shown in Fig 4a. The photographs are reproduced in Fig.4b, and are annotated with the time of exposure after discharge initiation.

They can be interpreted as follows. Immediately after initiation, a plasma was formed above the breech insulator and accelerated towards the muzzle of the gun. At 0.6 μs a second plasma began to form and this also accelerated away, at the end of the first half-cycle (1.0 μs). A third plasma then formed and this was ejected at the end of the second half-cycle (1.8 μs). Thus three discrete luminous plasmas were produced and accelerated. When the positions of their leading edges were plotted against time (Fig 5), it was noted that the first luminous front left the breech at 1.9 cm/μs, accelerated to 7 cm/μs while the second plasma was being formed, then later decelerated to 2 cm/μs as the second front moved from the breech. This unusual behaviour was also reported in another thruster, using PTFE propellant[17].

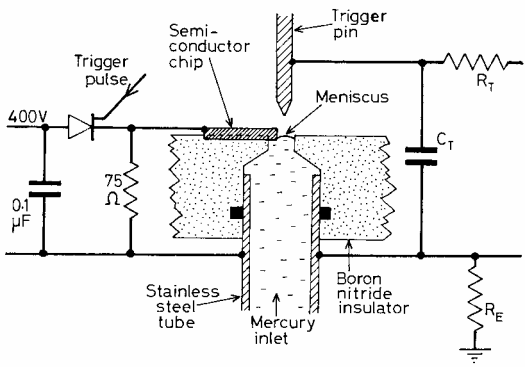

Figure 3. Configuration of two-stage triggering system.

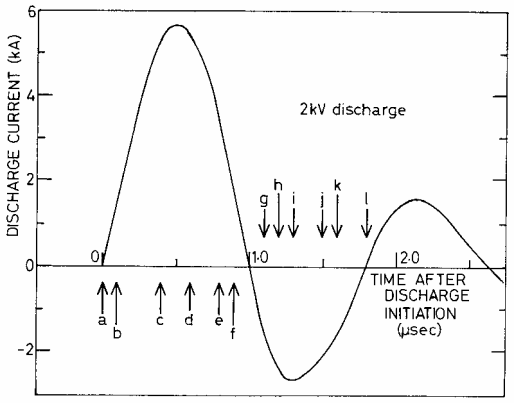

Figure 4a. Current waveform, showing times of photographs in Fig 4b.

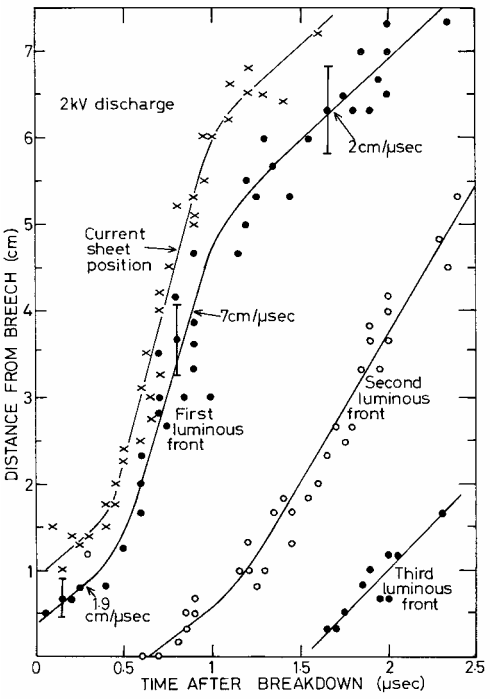

Figure 5. Plasma position as a function of time for luminous fronts.

Transverse and axial magnetic field components were also measured throughout the discharge at closely spaced intervals along the thruster axis, using a 1 mm diameter, 1 mm long probe coil containing 60 turns of wire. Typical results for the transverse component are shown in Fig 6. From these the position of the first current sheet was estimated as a function of time and, as shown in Fig 5, this behaved in a similar fashion to the first luminous front, although the former preceded the latter slightly, as found in other experimental arrangements[18].

These magnetic probe data allowed a qualitative analysis to be made of the evolution of the complex current system involving the separate plasmas, the electrodes and the discharge circuit (Fig 7). As the magnetic field was not zero at the instant of reversal of the discharge current, closed current loops flowed through the plasmas and these were included in this assessment.

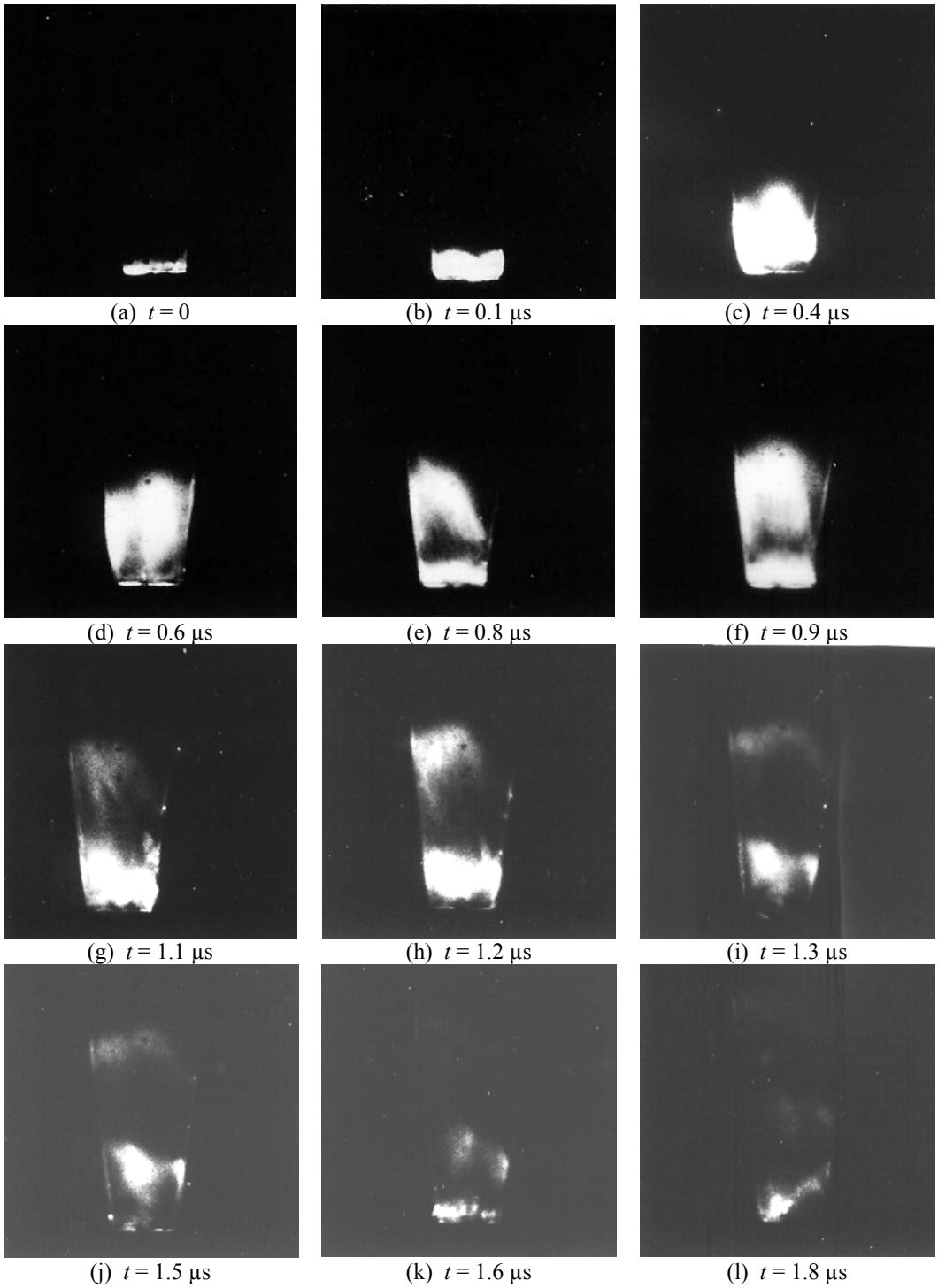

(a) $t = 0$ (b) $t = 0.1$ μs (c) $t = 0.4$ μs

(d) $t = 0.6$ μs (e) $t = 0.8$ μs (f) $t = 0.9$ μs

(g) $t = 1.1$ μs (h) $t = 1.2$ μs (i) $t = 1.3$ μs

(j) $t = 1.5$ μs (k) $t = 1.6$ μs (l) $t = 1.8$ μs

Figure 4b. Image converter photographs of the discharge up to 1.8 μs after initiation.

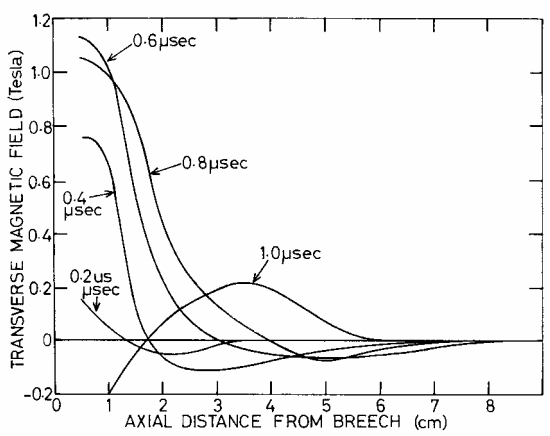

Figure 6. Transverse magnetic field distribution along the axis for times up to 1 μs after breakdown.

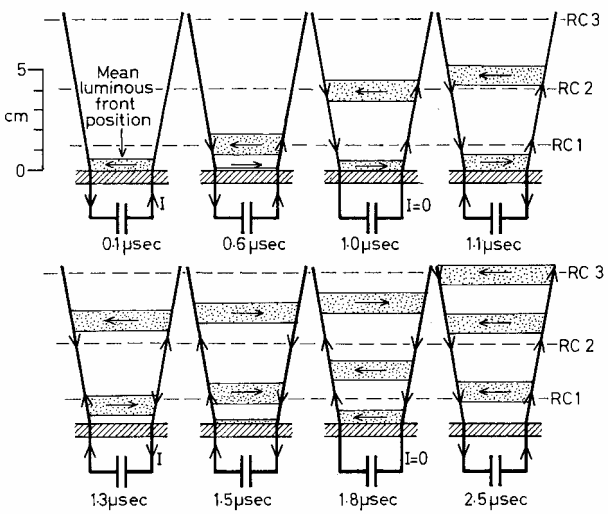

Figure 7. Discharge evolution as a function of time. RC1, RC2 and RC3 are Rogowski coil positions, and arrows indicate current directions.

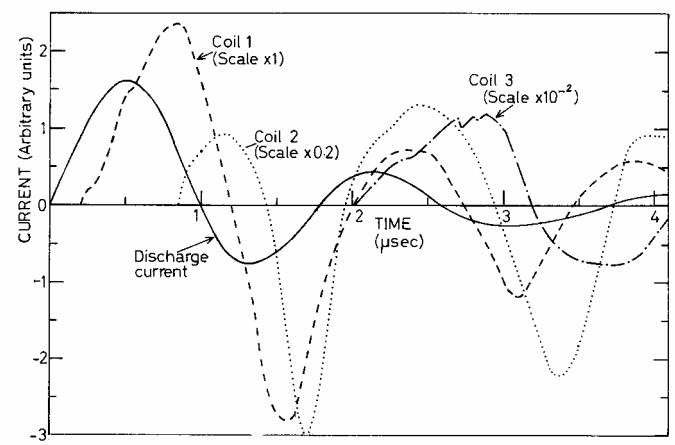

Figure 8. Relative outputs of Rogowski coils embedded in rail electrode.

Interactions between the magnetic fields produced by currents through individual plasmas were thought to cause the variable velocities[10] seen in Fig 5. It was therefore important to confirm the current system suggested in Fig 7. This was accomplished by burying three nominally identical miniature Rogowski coils in one electrode at positions 1.3, 4.1 and 7.6 cm from the breech. Although subjected to considerable electrical interference, these generally confirmed the analysis of the discharge evolution, with current reversals at the correct times and finite outputs when the main discharge current was zero (Fig 8). Absolute values of current were lower than expected, probably owing to the flow of a significant proportion through the boundary layers adjacent to the electrodes[19].

IV. Thrust Measurements

Although the photographs in Fig 4b gave an indication of the exhaust velocity, v, to be expected, and the mass of mercury injected by the triggering process had been measured, these data could not be used to estimate the thrust, T, and electrical efficiency, η_e, of the rail gun owing to uncertainty as to how much of the mass was accelerated. A thrust balance was therefore designed and used to determine the performance directly.

C. Design of the Thrust Balance

As the thruster was an impulse device giving an instantaneous thrust of perhaps 50 N for a time of less than 1 μs, an instrument for direct time-resolved measurements would have required a bandwidth of many MHz and linearity up to about 100 N. In addition, there were severe electrical noise problems, since the discharge was a powerful RF radiator; indeed, this was probably the most severe constraint on the actual thrust balance system design and

virtually precluded any attempt to achieve wide-band measurements. The alternative approach, employed in this work, was to determine the total impulse, *J*, by its effect on a dynamical system.

The thrust balance consisted of an aluminium alloy beam 70 cm long pivoted about a knife edge supported by a glass plate (Fig 9). The thruster was mounted on one end, the lightweight 1.33 μF capacitor on the other. The total weight was 2.77 kg and the period of oscillation 6.325 s. Electrical connections to components on the beam were made via contacts in mercury-filled pots positioned symmetrically about the pivot point to render surface tension effects negligible. The position of the centroid was adjusted by moving weight W1 along the beam axis and weight W2 vertically (Fig 9). The former adjustment balanced the beam into a horizontal position, while the latter was used to adjust the sensitivity. In the ideal situation of great sensitivity, yet adequate stability, the centroid was immediately below the pivot point. Electromagnetic damping was provided, but it was not often necessary to employ it.

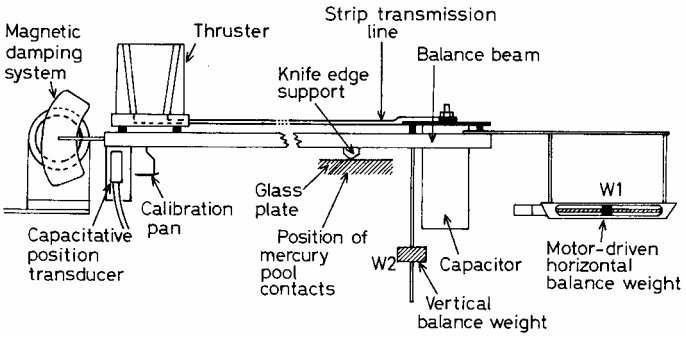

Figure 9. The thrust balance assembly.

The displacement of the balance was measured at the thruster end by a commercially available 'electronic micrometer'. This was a capacitative transducer operating in a 50 kHz bridge. The output of this instrument was externally filtered to remove the 100 kHz component introduced by rectification. It was amplified and filtered again by a fourth order Butterworth filter with a cut-off (-3 dB) at 3 Hz to remove low frequency noise transmitted through the building foundations and vacuum chamber. This noise, if present, sometimes had an amplitude considerably in excess of the signal due to the thruster.

On the most sensitive range, the system had a full scale deflection corresponding to a beam movement of 12.5 μm at the transducer. No day-to-day variation of the sensitivity was detected and results were reproducible within the resolution, which was 1% of full scale deflection.

D. Operation of the Balance

On firing the thruster, the impulse produced was transferred to the balance as an increase in angular momentum; it was therefore necessary to measure this immediately before and after the thruster was operated to determine *J*. In practice, the balance was initially at rest and the angular momentum after firing was deduced from the amplitude of the resulting oscillation. The dynamics of the system were analysed in detail, and it was shown that

$$J = \frac{W\Delta}{\omega\delta}$$

Here W is a calibrating mass at the thruster position causing a static deflection δ, Δ is the peak amplitude of oscillation, and the period is $2\pi/\omega$. In cases where damping was significant, it was necessary to determine its effect from the ratio of successive peaks of the waveform and make the appropriate correction when evaluating Δ. A typical output recording at maximum sensitivity is shown in Fig 10a. The large initial pulse was due to RF noise produced by the thruster; in this particular case, J = 1.11 ± 0.1 gs.

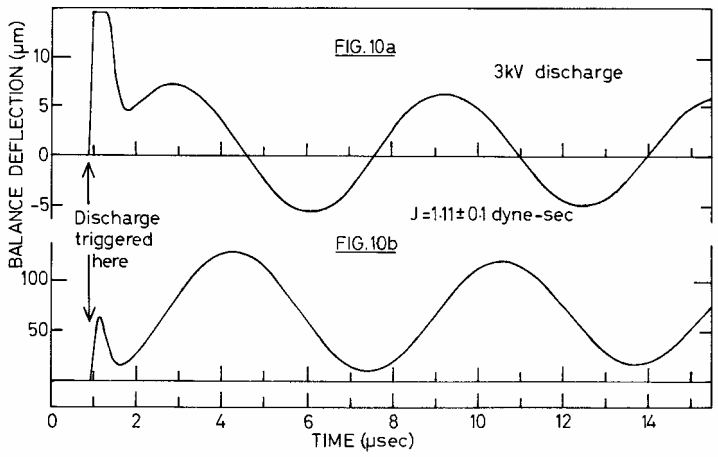

Figure 10. Records of thrust balance displacement with (a) rapid capacitor charging and (b) no recharging.

It was originally intended to operate the thruster repetitively at 10 to 20 Hz to integrate the individual impulses, thus giving a reading of continuous thrust. This, however, proved almost impossible because RF noise saturated the very sensitive electronics, despite double and in some cases triple screening. Furthermore, a local concentration of mercury vapour around the balance caused spurious breakdowns, severely affecting its equilibrium.

During operation of the balance in early experiments an unusual problem occurred. On firing the thruster, the zero of the balance shifted very rapidly by a large amount and this gave rise to cosinusoidal oscillations over an order of magnitude greater in amplitude than the sinusoidal response due to the thruster (Fig l0b). After eliminating electromagnetic and electrostatic forces acting directly on the balance, it was concluded from detailed analysis that electrostatic forces within the capacitor were pumping the oil during charging and discharging. There was thus a mass shift between these two states, which effectively applied a force to the balance. It was shown that the time constant of this phenomenon could be determined from the motion of the balance. It was established that this was about 0.25 sec, and it was therefore possible to eliminate the effect entirely by very rapidly re-charging the capacitor after firing the thruster. As this was done in 10 ms, the oil and centre of mass were unable to move before the electrostatic forces were re-applied.

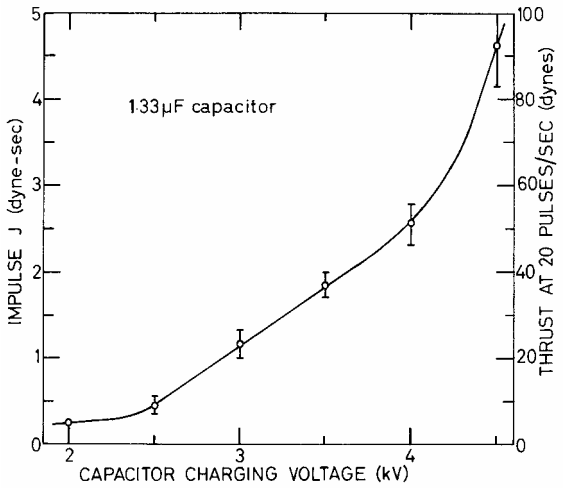

Figure 11. Impulse and thrust at 20 Hz as functions of charging voltage (1 mN = 100 dynes).

E. Impulse Measurements

Fig 11 shows the impulse obtained from the thruster as a function of charging voltage. The thrust at any pulse repetition frequency, f, was Jf; values for f = 20 Hz are shown. The design thrust of 0.5 mN (50 dynes) was attained at 10 Hz and 4.5 kV, or at 20 Hz and 4.0 kV, reflecting the rapid rise in J with voltage above 2.5 kV.

V. Exhaust Measurements

To obtain η_e from the thrust balance measurements, an independent determination of v was made using a Langmuir probe. To evaluate the mass utilisation efficiency, η_m, it was also necessary to determine the propellant consumption with the main discharge operating.

F. Langmuir Probe Measurements

A probe identical to that employed previously in the trigger plasma was placed in the exhaust from the thruster at various distances away from the breech. The same ion bombardment cleaning procedure was used as before.

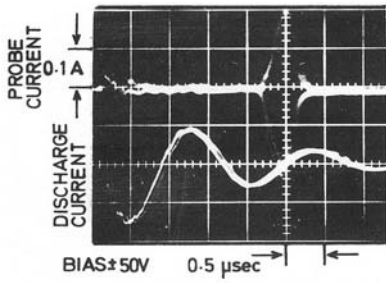

Figure 12. Overlaid Langmuir probe traces in the exhaust 20 cm from the breech.

The oscillograms of probe current (Fig 12) were single peaked and only of about 0.5 μs duration. There was no evidence of the structure expected from the image converter photographs (Fig 4b), even with very high amplification and slow sweep speeds. So it was concluded that only the initially accelerated plasma attained a sufficient density to be detectable. The velocities deduced from traces taken at different positions were also higher than expected from the photographs, that at 2.5 kV being, for example, 8 cm/μs. These values were close to the luminous front velocity of the first plasma between 1 and 5 cm from the breech (Fig 5), but did not agree with the luminous front velocity nearer the muzzle, where there was evidence of deceleration. This suggested that the luminous front merely marked the edge of the current sheet, which was retarded, but the high velocity plasma became decoupled from this and was able to escape from the thruster without significant loss of energy.

Voltage-current characteristics were reasonable in shape, although the data were rather scattered, and yielded values of T_e and n_e similar to those reported for other plasma guns[18,20]. For example, the characteristic in Fig 13, which was for the maximum points of the current traces at 2.5 kV and 20 cm from the breech, gave $T_e = 1.2 \times 10^5$ K

and $n_e = 2 \times 10^{14}$ cm^{-3}. It was shown that the plasma flow was sufficiently rapid to prevent the occurrence of serious plasma perturbations, so the values of n_e obtained were regarded as reasonably reliable.

Measurements were also made with the probe off-axis to determine the spatial extent of the exhaust. It was found, for example, that n_e was about 30% of its peak value 2 cm off-axis at a position 20 cm from the breech, in the plane of the electrodes. On the axis the value of n_e obtained with a 2.5 kV discharge was equivalent to a plasma density of $0.07/Z$ μg cm^{-3}, where Z is the mean ionic charge. Integrating n_e over the plasma volume, the total mass of the ionised component was very approximately $0.3/Z$ μg.

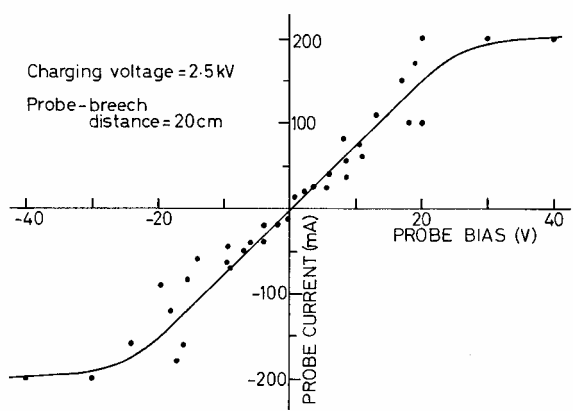

Figure 13. Probe current-voltage characteristic in the thruster exhaust.

G. Propellant Consumption

The propellant flow rate was measured by pulsing the thruster several thousand times, then determining the loss of mercury from a small reservoir placed in the breech for this experiment. As shown in Fig 14, the resulting values were much greater than those for the trigger discharge alone. At 2 kV the mass used per discharge was 13 μg and at 4 kV it was 58 μg; the trigger discharge produced 0.3 μg.

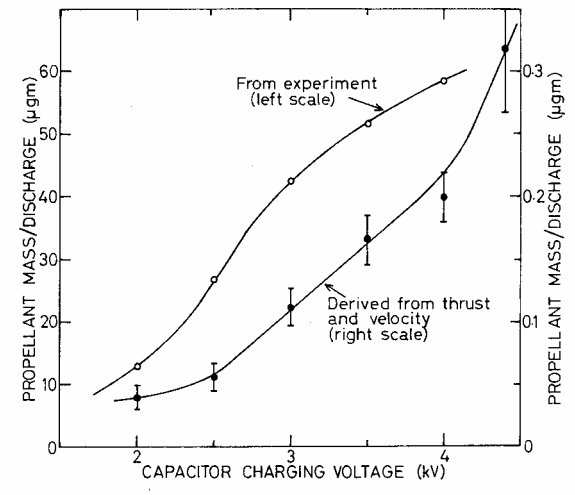

Figure 14. Directly measured and calculated propellant mass used per discharge as a function of charging voltage.

As it was not possible to explain this increase by evaporation[11], it was probably due to sputtering from the mercury meniscus by ions from the main discharge, especially during those periods when the plasma was close to the breech and local ion densities were high. It was shown[11] that the sheath at the meniscus probably had a potential in excess of 60 V across it. Ions accelerated by this would have caused severe sputtering, especially at high discharge voltages where both T_e and n_e would have been greater.

Evidence for the above mechanism was obtained using an image converter framing camera focussed on the breech region. This showed a bright streamer emanating from the mercury pool and extending axially between the electrodes as far as the rearmost plasma[11]. This was attributed to a local region of high density expanding towards the muzzle.

H. Calorimeter Experiment

To compare the performances of several different capacitor designs, a calorimeter was employed to indicate the energy content of the thruster exhaust. This device was made of 0.025 mm thick aluminium sheet and weighed 1.54 g. It was properly shielded externally and had a re-entrant conical end and adequate length to ensure that plasma was completely trapped within it[21]. Its temperature was monitored with a thermocouple and corrections were applied for heat losses.

It was found, as anticipated, that the capacitors with the lowest inductance and resistance gave the greatest calorimeter output, although low internal resistance appeared to be the more important parameter. Best results were achieved, by a factor of 30%, using an RAE-designed parallel plate capacitor with a strip transmission line outlet.

VI. Thruster Performance

Using values of v found with the Langmuir probe and using $J = mv$, the effective propellant mass, m, expelled per discharge was determined. This increased from 0.04 μg at 2 kV to 0.3 μg at 4.5 kV (see Fig 14), and was therefore much smaller than the total propellant consumption. Consequently η_m was only 0.2 to 0.5%. The values

of m were comparable with the 0.3 μg produced by the trigger discharge alone. It is therefore feasible that the initially accelerated plasma, which was the only one recorded by the Langmuir probe, consisted of a proportion of the trigger plasma only, and that all the propellant subsequently injected by the main discharge was wasted.

The values of m in Fig 14 were also less than those suggested by the Langmuir probe results. For example, at 2.5 kV, $m \sim 0.06$ μg, yet the probe gave $0.3/Z$ μg. Therefore, for agreement, $Z \sim 5$. Although errors were very large, it was thus inferred that the exhaust may have been multiply ionised, in agreement with data reported by Guman *et al*[17]. It was also concluded that fast neutral atoms must have contributed only slightly to the measured thrust.

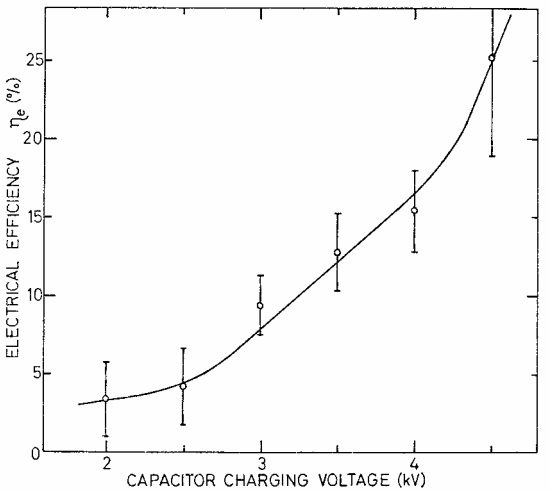

Figure 15. Electrical efficiency as a function of charging voltage.

The directed energy in the exhaust, $0.5mv^2$, was calculated from the above data and compared with the capacitor energy to give the values of η_e shown in Fig 15. These increased smoothly from 3% at 2 kV to about 25% at 4.5 kV and were comparable to those achieved by other plasma guns[8,18,22] operated in the same era.

VII. Conclusions

A pulsed plasma rail thruster, potentially capable of performing certain attitude control functions, was designed by the RAE in the late 1960s. It was unique in using mercury as the propellant. This device was successfully operated over a wide range of conditions, and its performance was studied extensively utilising a variety of diagnostic techniques, which would still be very useful today for an equivalent investigation.

In this thruster, an auxiliary discharge injected a small quantity of mercury propellant between the rail electrodes and ionised it, allowing the main oscillatory discharge to be initiated. Image converter photography and magnetic probes showed that a number of separate plasmas were accelerated towards the muzzle, and that interactions between them caused their velocities to be variable.

A sensitive thrust balance was used to determine the total impulse produced by the thruster at various capacitor charging voltages. The equivalent thrust with repetitive firing was, for example, 0.5 mN (50 dynes) at 10 Hz and 4.5 kV. Significantly, despite the optical evidence, a Langmuir double probe showed that the exhaust, some distance from the nozzle, consisted of a single high velocity plasma. Values of its velocity were combined with the impulse measurements to give the effective mass. This was comparable with the mass of mercury vapour produced by the trigger discharge, but far less than the total mass ablated from the mercury meniscus by ion bombardment during the main discharge. Clearly, the latter was not appreciably ionised or accelerated, and contributed little to the thrust, causing the mass utilisation efficiency to be very low, at 0.2 to 0.5%. The electrical efficiency was much greater, being 3% at 2 kV and 25% at 4.5 kV.

It was thus concluded that the thruster efficiently accelerated a large proportion of the mass injected by the trigger discharge to high velocity, but the very much greater quantity of propellant introduced by the main discharge was wasted. It is possible that this additional mass might be largely eliminated by using a rectangular pulse of current with a duration equal to the acceleration time of the first plasma, thus eliminating the subsequent plasmas and much of the sputtering of the mercury meniscus.

Acknowledgments

The bulk of the work reported here was performed by Jim Punter in the late 1960s and by Brian Barber in the early 1970s, both of whom made major contributions to understanding this complex device.

References

[1]Day, B P, Fearn, D G and Burton, G E, "Ion Engine Development at the Royal Aircraft Establishment, Farnborough", RAE Farnborough Technical Report TR 71102, May 1971.

[2]Fearn, D G and Smith, P, "A review of UK ion propulsion - a maturing technology", IAF Paper IAF-98-S.4.01, September/October 1998.

[3]Huddlestone, J, Wallace, N, de la Cruz, F and Smith, P, "An overview of the T6 gridded ion propulsion system pre-development activities for Alpha-Bus", Session 3NM1, *Proc 4th International Spacecraft Propulsion Conference*, Sardinia, 2-4 June 2004.

[4]Reader, P D, Nakanishi, S, Lathem, W C and Banks, B A, "A sub-milli-pound mercury electron-bombardment thruster", AIAA Paper 70-616, 1970.

[5]James, E, Dillon, T, Gant, G, Jan, L, Trump, G and Worlock, R, "A one millipound cesium ion thruster system", AIAA Paper 70-1149, 1970.

[6]Guman, W J and Nathanson, D M, "Pulsed plasma microthruster propulsion system for synchronous orbit satellite", *J Spacecraft and Rockets*, Vol 7, 1970, p 409.

[7]La Rocca, A V and Perkins, G S, "Pulsed plasma microthruster applications and techniques, AIAA Paper 68-554, 1968.

[8]Jarrett, O, Hoell, J M and Lockwood, D L, "Thrust measurements on a pulsed vacuum-arc thruster", AIAA Paper 70-1146, 1970.

[9]DeBra, D B, "Propulsion requirements for drag-free satellites", AIAA Paper 70-1145, 1970.

[10]Punter, T J, "Experimental results from a pulsed plasma accelerator with rail electrodes", RAE Technical Report 68277, 1968.

[11]Punter, T J and Fearn, D G, "An investigation of a combined discharge triggering and propellant injection system for use in a rail thruster", RAE Technical Report 71027, 1971.

[12]Fearn, D G and Wooding, E R, "Comparison of ion probe and double Langmuir probe measurements on plasma blobs", *Bull Am Phys Soc*, Series II, Vol 12, 1967, p 1160.

[13]Fearn, D G, "An investigation of the electrical breakdown of a plasma-electrode system", *J Phys D*, Vol 2, 1969, p 527.

[14]Nation, J A and Simpson, D, "A measurement of the effective thickness of the plasma sheath at a cold electrode", *Brit J Appl Phys*, Vol 16, 1965, p 1705.

[15]Waymouth, J F, "Perturbation of a plasma by a probe", *Phys Fluids*, Vol 7, 1964, p 1843.

[16]Zarabi, M J and Satyam, M, "The role of silicon carbide/mercury interface in ignitrons", *J Phys D*, Vol 3, 1970, p 1284.

[17]Guman, W J, Vondra, R J and Thomassen, K, "Pulsed plasma propulsion system studies", AIAA Paper 70-1148, 1970.

[18]Fearn, D G and Wooding, E R, "The conical z-pinch plasma gun", *Brit J Appl Phys*, Vol 18, 1967, p 213.

[19]Lovberg, R H, "The measurement of plasma density in a rail accelerator by means of Schlieren photography", *IEEE Trans Nucl Sci*, Vol NS-11, 1964, p 187.

[20]Vondra, R, Thomassen, K and Solbes, A, "Analysis of solid Teflon pulsed plasma thruster", AIAA Paper 70-179, 1970. *J Spacecraft and Rockets*, Vol 7, 1970, p 1402.

[21]Azovskii, Yu S, Guzhovskii, I T and Safronov, B G, "The measurement of the energy of plasma blobs by thermal probes", *Sov Phys - Tech Phys*, Vol 9, 1964, p 784.

[22]Gilmour, A S et *al,* "Recent progress in pulsed vacuum-arc microthruster research", AIAA Paper 68-555, 1968.